International Journal of Modern Physics C, Vol. 10, No. 8 (1999) 1399–1407

QUANTUM MONTE CARLO STUDY OF SITE-DILUTED HEISENBERG ANTIFERROMAGNET ON A SQUARE LATTICE

S. TODO*, K. KATO†, and H. TAKAYAMA

Institute for Solid State Physics, University of Tokyo
Tokyo 106-8666, Japan
**E-mail: wistaria@issp.u-tokyo.ac.jp*

K. HARADA

Department of Applied Analysis and Complex Dynamical Systems
Kyoto University, Kyoto 606-8501, Japan

N. KAWASHIMA

Department of Physics, Tokyo Metropolitan University
Tokyo 192-0397, Japan

S. MIYASHITA

Department of Applied Physics, University of Tokyo
Tokyo 113-8656, Japan

Received 28 September 1998

Ground-state phase transition of site-diluted Heisenberg antiferromagnets on a square lattice is studied. By using the continuous-time loop algorithm, we perform large-scale quantum Monte Carlo simulation on large systems at quite low temperatures. It is found that the critical concentration of magnetic sites is independent of the spin size S, and equal to the classical percolation threshold. However, the existence of quantum fluctuations makes the critical exponents deviate from those of the classical percolation transition. It is found that the transition is not universal, i.e., the critical exponents depend on the spin size S.

Keywords: Two-Dimensional Heisenberg Antiferromagnet; Site Dilution; Quantum Phase Transition; Percolation; Quantum Monte Carlo Method.

1. Introduction

Two-dimensional Heisenberg antiferromagnets (HAF's) have been studied extensively for the past few decades.[1] The main interest arises from its relevance to the high-temperature superconductivity in copper oxides,[2] because their parent

†Present address: Semiconductor Energy Laboratory Co., Ltd., Kanagawa 243-0036, Japan.

insulators are usually assumed to be described by the HAF on a square lattice. For the clean HAF, it is shown that the system exhibits long-range Néel order at the ground state,[3–5] although it has no long-range order at any finite temperatures.[6] The low-energy properties are successfully described by the field theoretical approach based on the quantum nonlinear σ model.[7,8]

Recently, effects of nonmagnetic impurities to the long-range order in the two-dimensional HAF have also attracted much interest.[11–14] In the classical limit, i.e., $S = \infty$, the site-diluted HAF at $T = 0$ becomes equivalent to the site-percolation model.[15] For the site percolation on a square lattice, the *percolation threshold*, which corresponds to the critical concentration of magnetic sites, is obtained as

$$p_{\mathrm{cl}} = 0.5927460(5) \tag{1}$$

by the most recent simulation.[16] At the percolation threshold, a second order phase transition occurs, which belongs to the same universality class as the $q = 1$ Potts model. For example, near p_{cl}, the staggered magnetization, or equivalently, the number density of magnetic sites belonging to the percolated cluster, vanishes as $M_s \sim (p - p_{\mathrm{cl}})^{\beta}$ with $\beta = 5/36$.[15]

For $S < \infty$, the classical percolation threshold p_{cl} still gives an *exact* lower bound for the critical concentration of the ground-state long-range order. One of the most important, but unsettled, questions is whether the existence of quantum spin fluctuations makes the critical concentration deviate form p_{cl}, or not.

In this paper, we report the results of large-scale quantum Monte Carlo (QMC) simulations on the site-diluted HAF on a square lattice. By using the continuous-time loop algorithm, we simulate quite large systems ($L \times L = 48 \times 48$) at very low temperatures ($T = 0.001$). It is found that the critical concentration (we refer to it as p^*) is equal to the classical percolation threshold p_{cl} for any spin size S.[14] Furthermore, it is found that the critical exponents, such as β, are not universal, i.e., their value significantly depends on S.[14]

The organization of the present paper is as follows: In Sec. 2, we describe our model and also our numerical method. In Sec. 3, we consider the $S = 1/2$ case. After presenting behavior of the spin-stiffness constant and the staggered magnetization in the weakly diluted region, we discuss the critical concentration and the critical exponents. In Sec. 4, we present our results for the higher-S cases ($S = 1$, $3/2$, and 2). We summarize our results in the final section.

2. Model and Numerical Method

The Hamiltonian of the site-diluted HAF is given by

$$\mathcal{H} = J \sum_{\langle i,j \rangle} \epsilon_i \, \epsilon_j \, \mathbf{S}_i \cdot \mathbf{S}_j \, . \tag{2}$$

Here, $\mathbf{S}_i = (S_i^x, S_i^y, S_i^z)$ denotes the quantum spin-S operator at site i, and the nearest-neighbor coupling constant is antiferromagnetic ($J > 0$). We assume $J = 1$

hereafter. The quenched dilution factors $\{\epsilon_i\}$ independently take 1 or 0 with probability p and $1-p$, respectively, where p denotes the concentration of magnetic sites. We consider $L \times L$ square lattices with periodic boundary conditions.

It is well known that traditional world-line Monte Carlo methods,[17] based on local updates of world line configuration, suffer from strong auto-correlation between successive configurations at low temperatures. This difficulty is shown to be overcome by the loop algorithm.[5,18,19] It reduces the auto-correlation time by orders of magnitude, and therefore makes it possible to perform highly reliable simulations on large lattices at extremely low temperatures. In the present simulation, we use the continuous-time loop algorithm[20] extended to general-S cases,[21–24] which works directly in the Trotter limit.

Another important feature of the present algorithm is its ergodicity; the winding number of world lines around vacant sites can change and the ground-canonical ensemble can be simulated. For each sample, 10^4 Monte Carlo steps (MCS) are spent for measurement after 10^3 MCS for thermalization. At each parameter set (L, T, p), physical quantities are averaged over $100 - 1000$ samples depending on L, T, and p.

3. Results for $S = 1/2$ Case

3.1. *Weakly diluted region*

In this section we consider the $S = 1/2$ case. First, we discuss the behavior of the spin-stiffness constant $\rho_s(p)$ and the staggered magnetization $M_s(p)$ in the weakly diluted region ($0.8 \leq p \leq 1$). The spin-stiffness constant is obtained by fitting QMC results for the correlation length to the low-energy asymptotic formula obtained by the chiral perturbation theory[8]

$$\xi(p,T) = g \exp\left(\frac{2\pi\rho_s}{T}\right)\left(1 - \frac{T}{4\pi\rho_s}\right), \tag{3}$$

where g is a p-dependent constant. We simulate rather large systems ($L \times L = 96 \times 96$ and 128×128) at a certain temperature region which satisfies $2 < \xi < 20$ ($0.3 \leq T \leq 0.5$ for $p = 1$, 0.975, and 0.95 and $0.2 \leq T \leq 0.4$ for $p = 0.875$). In this region, the QMC data for the two different system sizes coincide with each other besides statistical errors. For the clean case, we obtained $\rho_s(1) = 0.187(2)$, which agrees well with the previous estimates.[5,20]

The p-dependence of $\rho_s(p)$ is shown in Fig. 1. For $0.95 \leq p \leq 1$, one can see that $\rho_s(p)$ behaves as

$$\frac{\rho_s(p)}{\rho_s(1)} = (1 - R_\rho(1-p)) \tag{4}$$

with the initial reduction rate $R_\rho = 5.3$. The present estimate for R_ρ is clearly larger than that in the previous work ($R_\rho = 2$).[9] The reason for the disagreement might

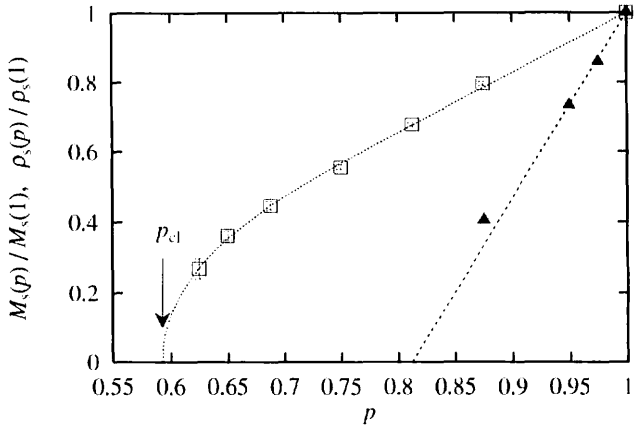

Fig. 1. Concentration-dependence of the spin-stiffness constant (solid triangles) and the staggered magnetization (open squares) for $S = 1/2$. Both quantities are normalized as unity at $p = 1$. The dashed line is obtained by the least-squares fitting for the spin-stiffness constant at $p = 1$, 0.975, and 0.95. The dotted line is a guide to eye.

be the smallness of the system size in the previous study. A naive extrapolation to $\rho_s = 0$ by using Eq. (4) gives $p = 0.81$ as an estimate for the critical concentration. The large initial reduction rate agrees quantitatively well with that of the Néel temperature of Zn-doped La_2CuO_4 observed by the recent NQR experiment.[10] However, the ρ_s at $p = 0.875$ has already started deviating from this formula (Fig. 1). The spin-stiffness constant should remain finite until the classical percolation threshold p_{cl}, because the antiferromagnetic long-range order exists for $p_{cl} < p \leq 1$ as discussed below.

The zero-temperature staggered magnetization $M_s(p)$ is calculated as

$$M_s^2(p) = \lim_{L\to\infty} \lim_{T\to 0} \frac{3S_s(L,T,p)}{L^d} \tag{5}$$

in terms of the static structure factor defined by

$$S_s(L,T,p) = \frac{1}{L^d} \sum_{i,j} e^{i\mathbf{k}\cdot(\mathbf{r}_i - \mathbf{r}_j)} \langle S_i^z S_j^z \rangle \tag{6}$$

at the momentum $\mathbf{k} = (\pi, \pi)$. Here, d is the spatial dimension ($d = 2$). The bracket in Eq. (6) denotes both of the thermal average and the average over samples. In the present simulation, we use an improved estimator to calculate $S_s(L,T,p)$, which reduces the variance of data greatly.

It should be noted that the order of the two limits in Eq. (5) is essential. To obtain the zero-temperature value of S_s at each p and L, we perform QMC simulations at low enough temperatures so that $S_s(L,T,p)$ exhibits no temperature dependence besides statistical errors.

In Fig. 2, we plot $S_s(L,0,p)/L^d$ against $1/L$. It is clearly seen that the data at each concentration fall on a straight line for large L. For the clean case ($p = 1$),

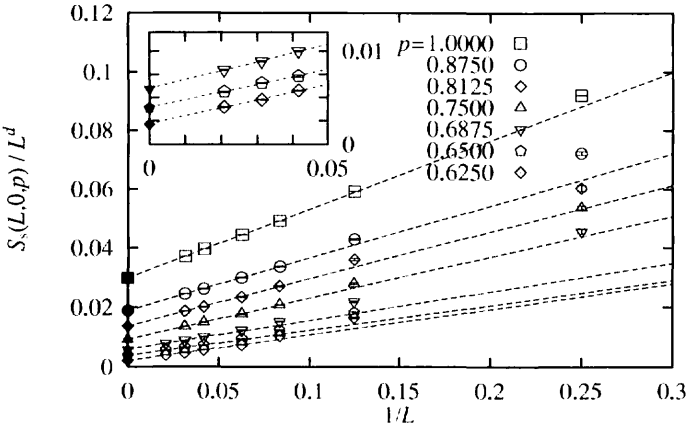

Fig. 2. System-size dependence of $S_s(L, T = 0, p)/L^d$ for $S = 1/2$. The dashed lines are obtained by least-squares fitting for the largest three system sizes for each p. The data with $p \leq 0.6875$ and $L \geq 24$ are also shown in the inset.

the leading finite-size correction is known to be of $O(1/L)$ according to the spin-wave theory.[25] The similar behavior for $p < 1$ indicates that there exists an antiferromagnetic long-range order with massless excitations, such as spin waves, even in the presence of impurities. The staggered magnetization in the thermodynamic limit is obtained by linear extrapolation in $1/L$ for the three largest system sizes at each p.

The staggered magnetization extrapolated to the thermodynamic limit is plotted in Fig. 1 as a function of p. We find that the initial reduction rate of staggered magnetization, R_m, is about 1.6, which is significantly greater than the classical case ($R_m = 1$).[15]

3.2. *Critical concentration and critical exponents*

In previous works, it was suggested that $p^* > p_{cl}$ for the present site-dilute model[11–13] and also for the bond-diluted model,[26] i.e., there exists a quantum disordered phase between p^* and p_{cl}. For example, $p^* = 0.655$ and 0.695 are obtained by the QMC simulation[11] and the analytic approach based on mapping to the nonlinear σ model,[13] respectively.

However, as is clearly seen in Fig. 2, the staggered magnetization at zero temperature remains finite even at $p = 0.625$. The possibility that p^* is greater than 0.625 is excluded definitely.[14] Note that as p decreases, the gap of a system of linear size L becomes smaller, and therefore lower temperatures are needed. For $p = 0.625$ and $L = 48$, T is taken as 0.002.

Compared to the previous estimates, our upper bound for p^* obtained above is very close to p_{cl}, which is an exact lower bound for p^*. Therefore, in the following, we assume $p^* = p_{cl}$ as a working hypothesis and verify it by performing a simulation just at $p = p_{cl}$.

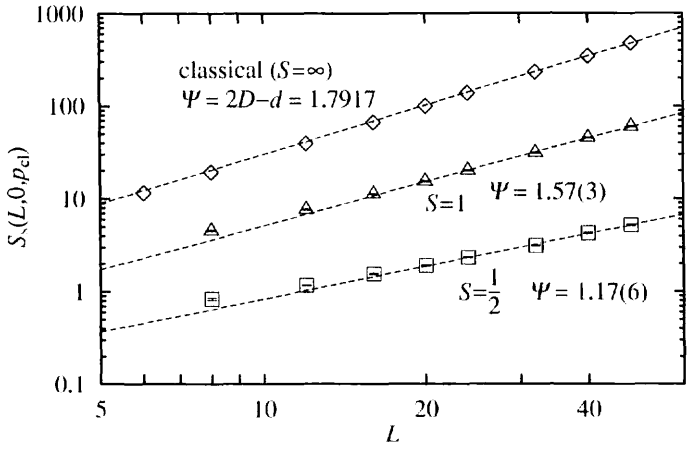

Fig. 3. System-size dependence of $S_s(L, T = 0, p)$ at $p = p_{cl}$ in the cases of $S = 1/2$ (squares) and $S = 1$ (triangles). The dashed lines are obtained by least-squares fitting for $L \geq 24$. The data in the classical limit are also plotted by diamonds.

In Fig. 3, we plot the system size dependence of $S_s(L, 0, p)$ just at the classical percolation threshold $p = p_{cl}$. For the largest size $L = 48$, we use $T = 0.001$ in order to estimate the zero-temperature value. We observe no tendency of saturation up to $L = 48$. Furthermore, the data for larger systems ($L \geq 20$) shows a clear power-law behavior

$$S_s(L, 0, p_{cl}) \sim L^{\Psi}, \tag{7}$$

which strongly supports our conjecture, $p^* = p_{cl}$.

The exponent Ψ in Eq. (7) is estimated as $\Psi = 1.17(6)$ by least-squares fitting for the data with $L \geq 24$. It should be emphasized that the value of Ψ definitely differs from that of the classical limit ($\Psi = 43/24 = 1.7917$). We also perform a scaling analysis including QMC data at high temperatures. We assume a usual algebraic scaling relation between the length scale and the energy scale

$$T \sim 1/L^z, \tag{8}$$

where z is the dynamical exponent. As shown in Fig. 4, $S_s(L, T, p_{cl})$ is well scaled by $\Psi = 1.27(2)$ and $z = 2.54(8)$. The value of exponent Ψ is slightly larger than the former estimate, but they agree satisfactorily with each other.

4. Results for Higher-S Cases

We perform similar analysis for $S = 1$, $3/2$, and 2 as in the previous section. In all the cases, the power-law behavior of the static structure factor is observed at $p = p_{cl}$. Thus, we conclude that $p^* = p_{cl}$ being independent of S.[14] For $S = 1$, the values of the exponent Ψ and z are estimated 1.57(3) and 1.58(10), respectively

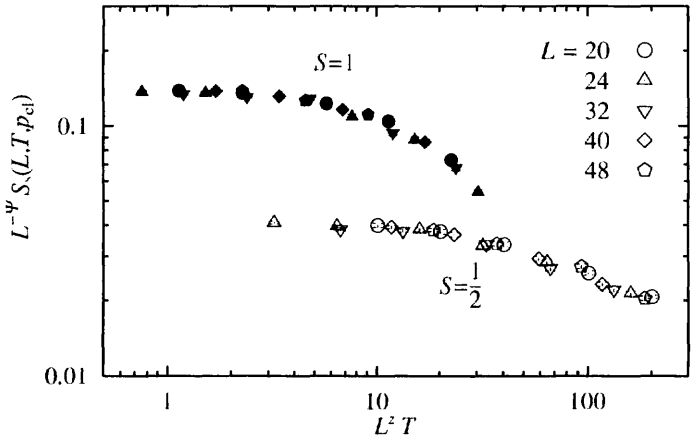

Fig. 4. Scaling plot of $S_s(L, T, p)$ at $p = p_{cl}$ for $S = 1/2$ and 1.

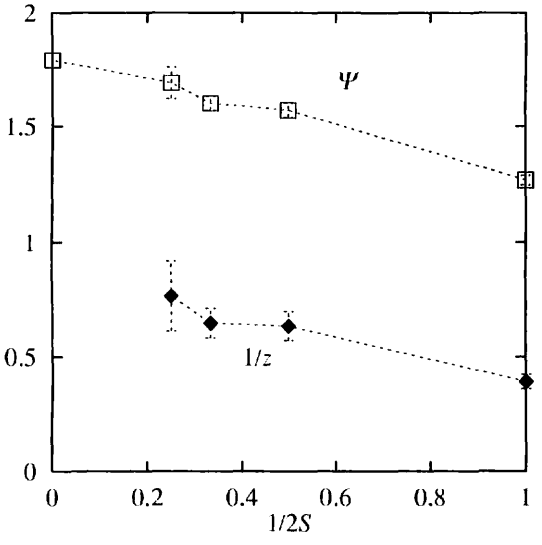

Fig. 5. S-dependence of the critical exponents Ψ (open squares) and $1/z$ (solid diamonds).

(Figs. 3 and 4). It should be emphasized that these estimates differ from those of the $S = 1/2$ case as well as of the classical case, i.e., these three cases belong to the different universality classes with each other. The S-dependence of the critical exponents are shown in Fig. 5. One can see a tendency such that the exponents depend on the value of S in the whole range of S, although we cannot conclude the nonuniversality between the $S = 1$ and $3/2$, or $S = 3/2$ and 2 cases in the present numerical accuracy.

5. Discussion

In the present paper, we have investigated the ground-state phase transition of the diluted HAF with $S = 1/2$, 1, 3/2, and 2. Contrary to the previous works,[11–13,26] our present QMC study has shown that the critical concentration is equal to the classical percolation threshold even in the $S = 1/2$ case.[a] On the other hand, it is found that the transition is nonuniversal; the critical exponents depend on the spin size S. This means that not only the fractal nature of the lattice geometry at $p = p_{\rm cl}$, but also the strength of the quantum fluctuation, controlled by the spin size S, are relevant in the present quantum phase transition. The criticality at $p = p_{\rm cl}$ might be characterized by an S-dependent exponent α, which is defined in terms of the staggered spin correlation function between two sites on a fractal cluster as

$$C(i,j) \sim r_{i,j}^{-\alpha} \quad \text{for } r_{i,j} \gg 1\,. \tag{9}$$

In the classical case, $C(i,j)$ takes a constant value, and therefore $\alpha = 0$. Together with the cluster-size distribution at $p = p_{\rm cl}$, predicted by the percolation theory,[15] we obtain a scaling relation between the S-dependent exponents Ψ and α:

$$\Psi = 2D - d - \alpha\,, \tag{10}$$

where D is the fractal dimension ($D = 91/48$).

For $p > p_{\rm cl}$, there exists a geometrical length scale $\lambda(p)$, which is defined as the average size of finite clusters. Because there exists a long-range order for $p > p_{\rm cl}$ as shown in the present paper, it seems natural to assume that there is no other macroscopic lengths scale, that is, the correlation length exponent ν is universal and equal to the classical value ($\nu = 4/3$).[14] The confirmation of this conjecture is now being proceeded and will be presented elsewhere.

Acknowledgments

Most of numerical calculations for the present work have been performed on the CP-PACS at University of Tsukuba, Hitachi SR-2201 at Supercomputer Center, University of Tokyo, and on the RANDOM at Materials Design and Characterization Laboratory, Institute for Solid State Physics, University of Tokyo. The present work is supported by the "Large-scale Numerical Simulation Program" of Center for Computational Physics, University of Tsukuba, and also by the "Research for the Future Program" (JSPS-RFTF97P01103) of Japan Society for the Promotion of Science. N.K.'s work is supported by Grant-in-Aid for Scientific Research Program (No. 09740320) from the Ministry of Education, Science, Sport and Culture of Japan.

[a]Quite recently, the $S = 1/2$ bond-diluted HAF on a square lattice is re-examined.[27] Contrary to the previous study,[26] the authors find that the critical concentration is equivalent to the percolation threshold, which is consistent with the present study. However, there remains a discrepancy in the value of the critical exponents.

References

1. For reviews, see e.g., E. Manousakis, *Rev. Mod. Phys.* **63**, 1 (1991).
2. J. G. Bednorz and K. A. Mueller, *Z. Phys. B* **64**, 189 (1986).
3. E. J. Neves and J. F. Perez, *Phys. Lett. A* **144**, 331 (1986).
4. J. D. Reger and A. P. Young, *Phys. Rev. B* **37**, 5978 (1988).
5. U.-J. Wiese and H.-P. Ying, *Z. Phys. B* **93**, 147 (1994).
6. N. D. Mermin and H. Wagner, *Phys. Rev. Lett.* **22**, 1133 (1966).
7. S. Chakravarty, B. I. Halperin, and D. R. Nelson, *Phys. Rev. B* **39**, 2344 (1989).
8. P. Hasenfratz and F. Niedermayer, *Phys. Lett. B* **268**, 231 (1991).
9. E. Manousakis, *Phys. Rev. B* **45**, 7570 (1992).
10. R. Carretta, A. Rigamonti, and R. Sala, *Phys. Rev. B* **55**, 3734.
11. J. Behre and S. Miyashita, *J. Phys. A: Math. Gen.* **25**, 4745 (1992); S. Miyashita, J. Behre, and S. Yamamoto, in *Quantum Monte Carlo Methods in Condensed Matter Physics*, ed. M. Suzuki (World Scientific, Singapore, 1994), p. 97.
12. C. Yasuda and A. Oguchi, *J. Phys. Soc. Jpn.* **66**, 2836 (1997); C. Yasuda and A. Oguchi, *J. Phys. Soc. Jpn.* **68**, 2773 (1999).
13. Y. C. Chen and A. H. Castro Neto, preprint (cond-mat/9903113).
14. K. Kato, S. Todo, K. Harada, N. Kawashima, S. Miyashita, and H. Takayama, preprint (cond-mat/9905379).
15. D. Stauffer and A. Aharony, *An Introduction to Percolation Theory* (Taylor and Francis, London, 1985), 2nd edition and references therein.
16. R. M. Ziff, *Phys. Rev. Lett.* **69**, 2670 (1992).
17. M. Suzuki, *Quantum Monte Carlo Methods in Condensed Matter Physics* (World Scientific, Singapore, 1994), and references therein.
18. H. G. Evertz, G. Lana, and M. Marcu, *Phys. Rev. Lett.* **70**, 875 (1993).
19. H. G. Evertz, in *Numerical Methods for Lattice Quantum Many-Body Problems (Frontier in Physics)*, ed. D. J. Scalapino (Perseus, Reading, 1999), and references therein.
20. B. B. Beard and U.-J. Wiese, *Phys. Rev. Lett.* **77**, 5130 (1996).
21. N. Kawashima and G. E. Gubernatis, *Phys. Rev. Lett.* **73**, 1295 (1994).
22. K. Harada, M. Troyer, and N. Kawashima, *J. Phys. Soc. Jpn.* **67**, 1130 (1998).
23. S. Todo, K. Kato, and H. Takayama, in *Computer Simulation Studies in Condensed-Matter Physics XI*, eds. D. P. Landau and H.-B. Schüttler (Springer-Verlag, Berlin, Heidelberg, 1999), p. 57.
24. S. Todo and K. Kato, preprint (cond-mat/9911047).
25. D. A. Huse, *Phys. Rev. B* **37**, 2380 (1988).
26. A. W. Sandvik and M. Vekić, *Phys. Rev. Lett.* **74**, 1226 (1995).
27. A. W. Sandvik, preprint (cond-mat/9909230).